The electrochemical reduction of Cr(VI) ions in acid solution at titanium and graphite electrodes

G. Velasco[1], S. Gutiérrez-Granados[2], C. Ponce de León[3], A. Alatorre[2], F.C. Walsh[3], I. Rodríguez-Torres*[,4]

[1] Minera San Xavier, 78440 Cerro de San Pedro, SLP, México
[2] Departamento de Química – División de Ciencias Naturales y Exactas, Universidad de Guanajuato, 36040 Guanajuato, GTO, México.
[3] Electrochemical Engineering Laboratory, Energy Technology Research Group, Engineering Sciences, University of Southampton SO17 1BJ, UK.
[4] Instituto de Metalurgia – Facultad de Ingeniería, Universidad Autónoma de San Luis Potosí, 78210 San Luis Potosí, SLP, México.

Abstract

Cyclic voltammetry (CV) and rotating disc electrode (RDE) linear sweep voltammetry were used to study the reduction of Cr(VI) ions on a titanium electrode at 298 K. Diffusion controlled reduction of Cr(VI) ions occurred between –0.22 V and –0.45 V *vs*. Ag/AgCl and appears to take place in a single, 3-electron step. The diffusion coefficient was 1.2×10^{-5} cm^2 s^{-1}, which agrees with data reported in the literature. Following a study in a three-electrode cell, the electrolysis of 2×10^{-3} mol dm^{-3} Cr(VI) in 0.1 mol dm^{-3} H_2SO_4 solution at –1.0 V *vs*. Ag/AgCl, on titanium and –0.65 V *vs*. Ag/AgCl on carbon electrodes were carried out. The area of the electrodes was 64 cm^2 and the mean linear flow velocity of electrolyte past the cathode varied between 10 and 80 cm s^{-1} (630 – 5680 cm^3 min^{-1}). The parasitic reactions of oxygen reduction and hydrogen evolution, which decreased the current efficiency, were observed during the reduction of Cr(VI) ions at titanium electrodes.

Key words: diffusion coefficient, graphite, hexavalent chromium; titanium

*Corresponding author. Tel: +52 444 8261450, Ext. 8236; Fax: +52 444 8254583.

E-mail address: learsi@uaslp.mx (I. Rodríguez)

1. Introduction

Over the last three decades, there has been a great deal of interest in technologies able to completely remove metal ions from wastewater and recover them in a usable form. Metals from valuable industrial waste solutions, such as those from the manufacture of catalytic converters, add value to the electrochemical process after been recovered but environmental concerns alone should be a sufficient driving force to remove them.

Due to its carcinogenic properties, the removal of Cr(VI) is particularly important [1]. In most countries, the disposal of hexavalent chromium and its compounds from industry into the environment is strictly regulated; reliable and safe technologies are required to recover or transform this metal ion into a less toxic product. Electrochemical methods are one of the greener options offering distinctive advantages relative to other technologies because the main reagent used is the electron, which is a clean reagent. One of the advantages is that frequently, the same reactor utilized for removal of ions can perform different electrochemical applications with only minor changes. Likewise, the applied potential or current, control the reaction rate and power losses can be minimized by appropriate cell design, including selection of electrode materials [2, 3].

The main sources of metals in wastewater are industrial processes such as electroplating, and metal extraction, production, treatment, etching, cleaning, finishing, recovery, or refining procedures. In rinse waters from chrome electroplating, the presence of others ions such as copper, zinc and iron are small compared with chromium (99%) which helps to improve the selectivity during recovery [4].

A number of studies of acid solutions containing Cr(VI) from the electroplating industry and their rinsing waters have been reported [5, 6]. These include the use of carbon [6-11], lead [12, 13], stainless steel [14], titanium [11, 14] and copper [15, 16] cathodes that have been used to directly or indirectly reduce Cr(VI) [2, 3, 17] present as the hexavalent chromium (dichromate) anion. The desired cathode reaction is the reduction of dichromate to chromic ions:

$$HCrO_4^- + 7H^+ + 3e^- \leftrightarrows Cr^{3+} + 4H_2O \qquad E^0 = 1.35 \text{ V } vs. \text{ SHE} \qquad (1)$$

However, hydrogen evolution occurs as a competitive, secondary reaction:

$$H_3O^+ + 2e^- \rightarrow H_2 + OH^- \qquad E^0 = 0.00 \text{ V } vs. \text{ SHE} \qquad (2)$$

Some authors have reported the precipitation of chromium compounds when carbon cathodes have been used without pH control [6-8]. There are also reports of low current efficiency for dichromate ion reduction [10] and passivation of the electrode surface [11] in gas diffusion electrode-packed bed electrode cell (GBC-cell) and a gas evolving rotating cylinder electrode cell [12]. The GBC-cell reactor combines a cathode consisted of packed bed carbon particles and a gas diffusion electrode to reduce chromate ions without external power source. Hydrogen gas is oxidised in the gas diffusion electrode while chromium ions spontaneously reduce on the carbon particles of the bed cathode. The attraction of this cell is that no electrical energy is necessary. Using the GBC-cell, Njau *et al.* [11] reported a current density ≈ 37.5 mA cm^{-2} during the reduction of Cr(VI) ions. The current density decreased slowly to 0.1 mA cm^{-2} after 1.6 hours of operation. When the cathode chamber consisted of a stack of

expanded titanium meshes, instead of carbon particles, the current decreased to ≈ 0.6 mA cm^{-2} and to 0.15 mA cm^{-2} after 4.5 and 18 hours operation, respectively. The authors suggested that the current drop was due to the formation of a 'passive inhibitor' species on the titanium surface but did not provide any experimental evidence. Chaudhary et al. [14] carried out the direct electrolysis reduction of Cr(VI) ions using titanium meshes at currents between 0.1 - 0.5 A during 5 hours, achieving almost 100% removal; no formation of passive compounds on the Ti electrode was reported. The data obtained with titanium [11, 13] are not conclusive since Njau *et al.* [11] reported problems of passivity without experimental evidence. Chaundary *et al.* [14] discarded titanium electrodes in favour of stainless steel ones that are easier to clean and handle.

When constant current or controlled electrode potential is applied to reduce Cr(VI), the pH gradually increases at the interface electrode-electrolyte due to hydrogen evolution in reaction (2). The hydroxyl ions can form an insoluble chromium hydroxide that passivates the electrodes. In order to avoid hydrogen evolution, lead rotating cylinder electrodes that have a high overpotential for hydrogen evolution in sulphuric acid solutions, have been used. The acid avoids the formation of chromium hydroxides on the cathode surface [12]. Although there is still some hydrogen evolution, the authors reported that the bubbles did not cover more than 3% of the electrode surface due to rotation of the electrode [12, 13]. However, the increase of parasite current due to proton reduction via reaction (2) at other electrodes, such as reticulated or porous carbon, could decrease the surface area available and increase ohmic drop [12].

Velasco *et al.*, [15] reported Cr(VI) reduction at copper cathodes with 70% conversion over 60 minutes, whereas Velazquez et al. [16] reported ≈100% conversion over 20 minutes. The studies did not take into account potential distribution over the electrode surface and it was suggested that some regions of the electrode did not reach the potential of Cr(VI) reduction and were not cathodically protected. This resulted in sections of the copper electrode at more positive potentials, forming a galvanic cell promoting copper dissolution:

$$HCrO_4^- + 3Cu^0 + 7H^+ \leftrightarrows Cr^{3+} + 3Cu^{2+} + 4H_2O \quad (3)$$

This reaction would cause high apparent electrochemical reaction rates of Cr(VI) reduction [18]. Although it is important to achieve high reaction rates, copper electrodes have the drawback of releasing unwanted copper ions into the solution. Further processing to remove the copper ions would lead to increased time and cost.

The aim of this paper is to show that under the appropriate conditions, titanium and graphite cathodes do not passivate during the reduction of hexavalent chromium ions, allowing a practical electrochemical process that can be developed for larger scale operations. The experimental conditions simulate those found in the rinse water produced from electroplating plants, which might typically consist of an aqueous solution containing 2×10^{-3} mol dm^{-3} Cr(VI) in 0.1 mol dm^{-3} H_2SO_4. The electrochemical techniques used in this paper are:

1) Cyclic voltammetry at static disc electrodes to evaluate the electrode potential range for Cr(VI) reduction and establish the general electrochemical characteristics,

2) Linear sweep voltammetry at a rotating disc electrode in order to quantify the mass transfer control conditions of the reduction rate of Cr(VI) ions at an appropriate electrode potential together with the diffusion coefficient in 0.1 mol dm^{-3} H_2SO_4 at 298 K.

3) Extended electrolysis of a known volume and concentration of Cr(VI) ions in order to establish the reaction kinetics by cathodic reduction including the mass transfer coefficient and the apparent first order rate constant that will enable the development of a scaled-up process.

2. Experimental details

2.1 Voltammetric studies

Cyclic voltammetry (CV) was used to evaluate the potential window of the reduction of Cr(VI). This technique allows to control the applied potential on the electrode surface as function of time (scan rate) and to determine quantitative kinetic data such as the diffusion coefficient. Linear sweep voltammetry (LSV) at the rotating disc electrode (RDE) allows mass transfer by diffusion and convection to be controlled and evaluated. These techniques allow the determination of electrode potential and hydrodynamic conditions that will facilitate efficient recovery of Cr(VI) at an acceptable rate during extended electrolysis.

Figure 1 shows the conventional glass, 3-electrode cell used for the static disk CV and RDE experiments. The solutions were prepared with deionised water (18 S cm^{-1}) and analytical grade $K_2Cr_2O_7$ adjusted at pH 1 with 98% H_2SO_4. Nitrogen gas (99.99%) was bubbled through the solution for 15 minutes to remove dissolved oxygen before the electrochemical experiments. The working electrodes were prepared in the laboratory by inserting a titanium bar of 3 mm diameter into a PTFE sleeve of 10 mm diameter with a central hole of 3 mm

diameter. This resulted in a well-sealed working electrode with an exposed area of 0.0707 cm^2. The surface of the electrodes was polished with wet alumina powder of 1.0, 0.5 and 0.01 μm grade, followed by rinsing with deionised water and 1-minute immersion in water in an ultrasonic bath to remove alumina residues. A 0.5 mm diameter, 5 cm long platinum wire was used as the counter electrode while the reference electrode was Ag/AgCl (saturated KCl). The electrochemical studies were carried out at 298 K with an EG&G 273A potentiostat and EG&G 636 rotating disc electrode at rotation rates of 200 to 3600 rpm.

2.2 Extended electrolysis studies

These experiments facilitated calculation of performance indicators such as current efficiency, space-time yield, normalized space velocity and specific energy consumption of the reduction of chromium under mass-transfer control in an electrochemical reactor. Solutions containing 2×10^{-3} mol dm^{-3} Cr(VI) were prepared from analytical grade $K_2Cr_2O_7$ (KEM) in 0.1 mol dm^{-3} H_2SO_4 (Baker) using deionised water. Linear sweep voltammetry experiments were conducted to obtain current density *vs*. electrode potential curves in a filter press electrochemical reactor (FPER) built in the laboratory and shown in Figure 2. This reactor is similar to the FM01-LC reactor [19] and consisted of two acrylic frames holding a PTFE spacer of approximately 25 × 6 × 0.5 cm with a hollow area of 16 × 4 cm in the center forming a rectangular flow electrolyte compartment. The spacer included flow distributors at both ends of the 16 cm length and the anode and cathode electrodes face each other at each side [15]. The electrodes consisted of a titanium plate cathode of 16 × 4 cm with projected 64 cm^2 active area and a platinized-titanium plate counter electrode of the same dimensions while the reference electrode was Ag/AgCl. The reference was connected to a Luggin

capillary located near the cathode surface, via a flexible transparent tubing (Tygon® Lab R-3603, with an ID of 1.6 mm) inserted on the wall of one of the spacers. The reference electrode compartment contained saturated KCl solution. The anode-cathode separation was 0.3 cm fixed by PTFE spacers and gaskets. The polarization curves and the electrolysis experiments were carried out at volumetric flow rates within the range of 630 to 5680 cm^3 min^{-1}, which correspond to a mean linear flow velocity of 10 to 80 cm s^{-1}, respectively. A magnetically coupled drive pump (March 320 AP MD) and a RMB 85 Dwyer flow meter were used to pump and measure the flow rate of the electrolyte. The solutions were recirculated through a 2 dm^3 glass reservoir equipped a double jacket wall to hold water at 298 K in a batch recirculation mode of operation. The water temperature was controlled with a stainless steel water-cooling coil [15].

A d.c. power source (Zurich DS-304M) was used for the electrolysis. The data was acquired through a multimeter (Steren MUL-600) connected to a PC via a RS232 electronic interface. Aliquots of 1 cm^3 were taken from a 1.5 dm^3 solution of electrolyte at regular intervals of time to measure the concentration of Cr(VI) with a Spectronic 3000 UV-Vis spectrophotometer at 350 nm wavelength. The total concentration of metallic chromium ions was determined by a Perkin Elmer Analyst model 200 atomic absorption spectrophotometer equipped with an air-acetylene or nitrous oxide-acetylene flame at a wavelength of 357.9 nm.

3. Results and discussion

3.1 Voltammetry at a titanium electrode

Figure 3 shows the cyclic voltammetry of Cr(VI) ions at a titanium disc electrode at concentrations of 4, 12 and 20 × 10^{-3} mol dm^{-3} in a oxygenated solution. Peak I occurs at an

electrode potential of approximately –0.45 V *vs.* Ag/AgCl, and represents the reduction of the hexavalent chromium ion according to reaction (1) [18]. The peak current increases with the concentration of Cr(VI) and occurs just before the oxygen reduction reaction (ORR) (4), at –0.64 V *vs*. Ag/AgCl [16], which can only be observed in the background current (process II) as a very small bump in the forward scan:

$$O_{2(aq)} + 4H^+ + 4e^- \leftrightarrows 2H_2O \qquad E^0 = 1.229 \text{ V } vs. \text{ SHE} \qquad (4)$$

During the reverse scan, there is no oxidation peak within the electrode potential window used in this study suggesting an irreversible process on titanium electrode. The oxidation of Cr(III) might occur together with the oxygen evolution at more positive potentials which were not investigated in this process. The results in a deoxygenated solution (not shown) during the electrolysis of Cr(VI) ions show no passivation of the titanium electrode surface. However, in the presence of oxygen, the reduction might cause low current efficiency and selectivity since the reduction potentials of Cr(VI) ions and dissolved O_2 are close.

Cyclic voltammetry was carried out at linear potential sweep rates between 20 and 200 mV s^{-1} (not shown) for the reduction of 2×10^{-3} mol dm^{-3} Cr(VI) ions on the titanium electrode in deoxygenated and non-deoxygenated 0.1 mol dm^{-3} H_2SO_4 solutions. Figure 4 shows the peak current density versus the square root of the scan rate in the presence and in the absence of oxygen. The curves show clearly the influence of oxygen on the limiting current values. The diffusion coefficient of Cr(VI) ions calculated from the slope in the absence of oxygen was 1.87×10^{-5} cm^2 s^{-1}. The diffusion coefficient is similar to the one obtained using a rotating disc electrode reported in the following section and the line pass through (0,0). In

the presence of oxygen, the curve does not pass through the origin due to oxygen reduction accompanying Cr(VI) ion reduction. The linear behaviour in both cases shows that the reduction of Cr(VI) ions on a titanium surface occurs in a single stage by a diffusion controlled process unlike the reduction on vitreous carbon electrode where the process occurs in two stages; adsorption followed by reduction [20].

The voltammetric studies indicated that the electrochemical reduction of Cr(VI) on titanium is a single irreversible process controlled by mass-transfer. When using oxygenated solutions, there was a slight drop in current efficiency but passivation, leading to abrupt decrease in the current was not observed over the potential range studied.

3.2 Rotating disc electrode

Figure 5 shows the reduction of 2.0×10^{-3} mol dm^{-3} Cr(VI) ions in H_2SO_4 0.1 mol dm^{-3} at a titanium rotating disc electrode of 0.07 cm^2 area, in the presence and in the absence of oxygen. The comparison of the two systems at the same rotation rate shows the influence of the presence of oxygen. In the kinetic and mixed control regions between –0.2 V and –0.55 V *vs*. Ag/AgCl, the current at all rotation rates in the presence of oxygen is slightly higher than in its absence and seems to increase with the rotation rate. An inclined limiting current 'plateau' can be observed in the presence of oxygen while a flatter limiting current plateau is observed when oxygen was removed from the electrolyte. The increment of the limiting current plateau is proportional to the square root of the rotation rate of the electrode which suggests that the reduction of Cr(VI) ions under these conditions is mass transfer controlled. The mass transfer controlled region at which the limiting current plateau appears in a deoxygenated solution is < 300 mV wide.

Similar rotating disc electrode experiments to those shown in Figure 5 were carried out at different concentrations of Cr(VI) ions in the absence of oxygen. Figure 6 presents a Levich plot of limiting current density j_L, versus the square root of the rotation rate $\omega^{1/2}$ at different Cr(VI) ion concentrations. The linearity of these curves through the origin confirms that the reduction is a mass transfer controlled process between Cr(VI) concentrations of 1×10^{-3} mol dm^{-3} and 3×10^{-3} mol dm^{-3} and rotation rates of 400 to 3600 rpm. The Levich equation:

$$j_L = 0.62nFD^{2/3}\upsilon^{-1/6}c\omega^{1/2} \quad (5)$$

where n is the number of electrons interchanged, F the Faraday constant, D the diffusion coefficient, υ the kinematic viscosity, c the concentration of Cr(VI) ions, and ω the angular rotation velocity of the electrode, was used to calculate the diffusion coefficient of Cr(VI) from the slope of each line: The value of the diffusion coefficient D_{HCrO4^-}, was $(1.2\pm0.1) \times 10^{-5}$ cm^2 s^{-1}, which is similar to that reported in the literature of 1.1×10^{-5} cm^2 s^{-1} [14] and 1.326×10^{-5} cm^2 s^{-1} at a Cr(VI) concentration of 5×10^{-3} mol dm^{-3} reported in [20].

When titanium was used as a working electrode, the oxidation of Cr(III) ions could not be observed after the reduction process over the range of potentials studied. The low current efficiencies and long electrolysis times reported in the literature when titanium has been used as a working electrode [11, 13] are attributable to unwanted oxygen reduction and hydrogen evolution as parasitic cathodic processes, having a negative effect on the current efficiency and energy consumption, rather than on electrode passivation.

3.3 Linear sweep voltammetry on titanium and carbon electrodes

Figure 7 shows the current density *vs.* potential curves during the reduction of 2×10^{-3} mol dm^{-3} of Cr(VI) (100 mg dm^{-3}) in 0.1 mol dm^{-3} H_2SO_4 solution on a titanium plate and on a graphite plate on the FM01 like reactor. The electrodes were 64 cm^2 area and the experiment was carried out from 10 to 80 cm s^{-1} mean linear velocity in the presence of oxygen. The curves at the titanium electrode are similar to those obtained by Velasco et al. [15] who used a copper disc electrode and found that the process was mass transfer controlled, being affected negatively by O_2 reduction and H_2 evolution. The open circuit potential on the titanium electrode was approximately –0.5 V *vs*. Ag/AgCl and the limiting current density region within the region of –1.0 V to –1.2 V *vs.* Ag/AgCl. The increase of the current density with the mean linear flow velocity in the polarization curves suggests that there is no passivation of the titanium electrode surface. The experiment was repeated in triplicate and the same current was observed.

In the case of the graphite electrode, the open circuit potential was around +0.4 V *vs*. Ag/AgCl which is 0.9 V more positive than the potential observed at the titanium electrode. The curves are characterised by a gradual current increase from the start possible due to the oxygen reduction reaction, with no clear limiting current plateau except for the lowest mean linear flow velocity at 10 cm s^{-1} that forms a vague plateau region. The limiting current could be taken approximately between –0.4 and –1.0 V *vs*. Ag/AgCl. This agrees with the other works where the reduction of Cr(VI) ions on graphite electrodes occurred at potentials more negative than –0.6 V *vs*. Ag/AgCl [15]. Considering this, the limiting current value could be evaluated at –0.65 V *vs.* Ag/AgCl. As the mean linear velocity increased, the curves becomes steeper and with no defined limiting current region that seems to be dependent by the ohmic

drop especially at a mean linear rate of 80 cm s^{-1}. The polarization curves demonstrate a mixed control for the hexavalent chromium reduction, analogous behaviour to that observed by Velasco *et al.* who used a vitreous carbon electrode [20].

LSV experiments show that for both electrodes the mean linear flow velocity increases the current density, indicating the mass-transfer control dependence of the reduction of Cr(VI).

3.4 Electrolysis at titanium and graphite electrodes

Constant potential electrolysis of Cr(VI) ions was carried out at the electrode potentials selected within the limiting current region observed in the linear sweep potential curves. An electrode potential value of –1.0 V *vs*. Ag/AgCl was selected for the electrolysis with the titanium electrode, whereas –0.65 V *vs*. Ag/AgCl for the graphite electrode. The cell voltage and current were followed in order to calculate the energy and current efficiency

The limiting current density j_L, on a graphite electrode in figure 7, does not exhibit linear behavior with the square root of the mean linear flow velocity since the process is not only mass transfer controlled but also has the ORR influence. The increase in current density j from 60 to 80 cm s^{-1} is of minor significance compared to the increase from 10 to 25 cm s^{-1}. Although it is difficult to establish the range of electrode potentials where oxygen reduction and hydrogen evolution do not affect the current efficiency and selectivity, the electrolysis was carried out by controlling the cell voltage between 2.3 – 2.5 V in order to maintain the graphite electrode potential at –0.65 V *vs*. Ag/AgCl.

In the case of a titanium cathode, a cell voltage between 1.9 – 2.0 V was required to maintain the electrode potential at –1.0 V *vs*. Ag/AgCl. It is worth noting that at an applied cell voltage

of 1.9 V (–1.0 V *vs.* Ag/AgCl) and a mean linear flow rate of 10 cm s^{-1} corresponds to the region where ORR takes place and a lower current efficiency for Cr(VI) reduction, compared to other linear flow rates studied during the electrolysis, would be expected.

From the electrolysis experiments of 2×10^{-3} mol dm^{-3} of Cr(VI) in 0.1 mol dm^{-3} H_2SO_4 at constant voltage, the conversion percentage against the mean linear flow velocity after 60 minutes electrolysis is plotted in Figure 8 for graphite and titanium cathodes. When a graphite electrode was used, the depletion of Cr(VI) was 21% and 49% at a mean linear flow rate 10 and 80 cm s^{-1}, respectively. The data from the figure suggest that at linear flow rates above 60 cm s^{-1}, Cr(VI) conversion does not increase. These results confirm that the reduction of Cr(VI) is under mixed control as was identified through the polarization curves in microelectrolysis studies using this material [14]. When a titanium electrode was used, conversions between 18% and 41% of Cr(VI) in 60 minutes, at mean linear velocities of 10 and 80 cm s^{-1}, respectively were observed. The conversion rate for titanium is lower than that obtained for graphite, 41% and 49% respectively, even when a high electrolysis cell voltage was applied (2.4 V). The lower conversion rate may be due to ORR, which lowers the selectivity and the current efficiency.

The results of the electrolysis experiments at more than 60 minutes confirmed that no passivation occurred. The electrochemical reduction of Cr(VI) ions on a graphite electrode during the electrolysis was both, charge and mass transfer controlled process whereas for titanium electrode, the oxygen evolution reaction decreases the current efficiency. Over a long electrolysis time, the influence of oxygen evolution will increase as the concentration of chromium ions becomes lower.

The mass transfer coefficient (k_m) for Cr(VI) reduction can be determined by applying a model for electrochemical reactors operating under a batch mode, equation (6) below. The equation assumes that the decay of Cr(VI) ions concentration follows first order reaction kinetics [21-23]:

$$\ln\left(\frac{c_t}{c_0}\right)=\left(-\frac{Ak_m}{V_S}\right)t=-mt \tag{6}$$

where c_t and c_0 are the concentrations of Cr(VI) ions at time t and initial, respectively, A is the electrode area, k_m is the mass transfer coefficient, V_S is the constant volume of the electrolyte in the reservoir and m is the slope of the semilogarithmic plot of (c_t/c_0), *vs* t. The model applies when the transfer of reactive ions occurs under convective-diffusion control and in this case, it was used to calculate the value of the mass transfer coefficient, k_m from the slopes at each flow rate. The mass transfer coefficient values for the graphite and titanium electrodes are in the order of (1×10^{-3} to 6×10^{-3}) cm s^{-1} (see Table 1), similar to those reported for the characterization of filter press type electrochemical reactor with the redox pair $Fe(CN)_6^{3-}$/ $Fe(CN)_6^{4-}$ which is a fast and reversible system [23].

The current efficiency (ϕ) defined as the ratio between the theoretical charge (q) required for a specific reaction and the total or real charge (q_{Total}) transferred through the electrode was evaluated through equation 7. The value of q_{Total} was obtained by integrating the current *vs*. time curve and electrical charge required to electrochemically reduce a certain amount of Cr(VI) used Faraday's law:

$$\phi = \frac{q}{q_{Total}} \tag{7}$$

The current efficiency (ϕ) when a graphite electrode was used was nearly 100% over the entire flow studied range (see Figure 9), which corroborates that an optimal electrolysis voltage has been selected for Cr(VI) reduction on this electrode. The current efficiency when a titanium electrode was used increases from 67% to 83% with a proportional increase observed with respect to the mean linear fluid velocity. These results corroborate the hypothesis generated in the analysis of the electrolysis current density *vs.* potential, where the problem of the reduction potential of oxygen and of the medium being too close to the electrode potential reduction of Cr(VI) was posed in the case of titanium electrode.

Figure 9 also shows the energy consumption after 60 minutes electrolysis. On the graphite electrode, the energy consumption is practically constant at 16 kW h mol^{-1} at all the flow rates while in the case of titanium the energy consumption is slightly higher from 29 kW h mol^{-1} at low mean linear flow rates to 23 kW h mol^{-1} at the highest flow rate. The energy consumption on a titanium electrode is greater than that with the graphite electrode because of the higher overpotential linked to Cr(VI) reduction and the nearness of secondary reactions, i.e. the oxygen reduction and hydrogen evolution reactions that decreases the selectivity of the process. The energy consumption of this work are lower than other processes used to reduce chromium from solution, for example the reduction of 5 mg dm^{-3} Cr(IV) via a photocatalytic method that required 7590 and 3370 kW h mol^{-1} at 20 ºC and 35 ºC, respectively [24]. Another example is an electrocoagulation process that required 11.9 kW h mol^{-1} [25]; although the energy consumption in this process is of the same order of

magnitude as in the work presented in this paper, the drawback of the electrocoagulation method is that the chromium specie remains as Cr(VI) even if it is removed from solution.

Conclusions

Graphite and titanium electrodes do not exhibit surface passivation during the electrolysis to reduce hexavalent chromium ions. The analysis of the reaction through polarization curves enabled the determination of the electrode potential conditions to carry out a constant potential electrolysis for the electroreduction of Cr(VI).

Direct reduction of Cr(VI) at graphite occurs with greater efficiency and lower energy consumption than on titanium, although the Cr(VI) concentration still remains above the limits specified by environmental regulations. To obtain concentrations below these limits, the electrode area should be increased by the use of three-dimensional electrodes.

In the case of titanium, there is a higher overpotential for Cr(VI) reduction; $O_{2(aq)}$ reduction and $H_{2(g)}$ evolution occur at very close potentials, which leads to lower current efficiency and slightly high energy consumption.

This work demonstrates that titanium and graphite electrodes can be used to reduce Cr(VI) using an electrochemical reactor at constant potential, in the acidic conditions typically used in the electroplating industry, with a much lower energy consumption than other processes.

Acknowledgements

The authors gratefully acknowledge financial support provided by the Secretary of Public Education (SEP) PRODEP redes CAs programme.

REFERENCES

1 R.M. Sedman, J. Beaumont, T.A. McDonald, S. Reynolds, G. Krowech, R. Howd. "Review of evidence regarding the carcinogenicity of hexavalent chromium in drinking water." *J Environ Sci Health C Environ Carcinog Ecotoxicol Rev*., 24 (2006) 155 – 182.

2 F.C. Walsh. "Electrochemical technology for environmental treatment and clean energy conversion". *Pure Appl. Chem.*, 12 (2001) 1819 – 1837.

3 D. Pletcher, F.C. Walsh, Industrial Electrochemistry, 2nd edn., Chapman and Hall, London, (1990); ISBN 0-412-30410-4; softcover version, Blackie Academic & Professional, Glasgow, (1993); ISBN 0-7514-0148.

4. A. Agrawal, V. Kumar, B. D. Pandey. "Remediation options for the treatment of electroplating and leather tanning effluent containing chromium - a review". *Miner. Process. Extr. Metall. Rev.*, 26 (2005) 99 – 130.

5 C.E. Barrera-Díaz, V. Lugo-Lugo, B. Bilyeu. "A review of chemical, electrochemical and biological methods for aqueous Cr(VI) reduction". *J. Hazard. Mater.*, 1 – 12 (2012) 223-224.

6 M. Owlad, M.K. Aroua, W.A.W. Daud, S. Baroutlan. "Removal of hexavalent chromium-contaminated water and wastewater: A review". *Water Air Soil Pollut*, 200 (2009) 59 – 77.

7 D. Golub, Y. Oren. “Removal of chromium from aqueous solutions by treatment with porous carbon electrodes. Electrochemical principles”. *J. Appl. Electrochem.,* 19 (1989) 311 – 316.

8 M. Abda, Z. Gavra, Y. Oren. “Removal of chromium from aqueous solutions by electrochemical treatment on fibrous carbon and graphite electrodes: Column Effects”. *J. Appl. Electrochem.,* 21 (1991) 734 – 739.

9 E.P.L. Roberts, H. Yu. “Chromium removal using a porous carbon felt cathode”. *J. Appl. Electrochem.,* 32 (2002) 1091 – 1099.

10 F. Rodríguez-Valadez, C. Ortiz-Éxiga, J. G. Ibáñez, A. Alatorre-Ordaz, S. Gutiérrez-Granados. “Electroreduction of Cr(VI) to Cr(III) on Reticulated vitreous carbon Electrodes in a parallel-plate reactor with Recirculation”. *Environ. Sci. Tech.,* 39 (2005) 1875 – 1879.

11 K.N. Njau, L.J.J. Janssen. “Electrochemical reduction of chromate ions from dilute artificial solutions in a GBC-reactor”. *J. Appl. Electrochem.,* 29 (1999) 411 – 419.

12 A. Radwan, A. El-Kiar, H.A. Farag, G.H. Sedahmed. “The role of mass transfer in the electrolytic reduction of hexavalent chromium at gas evolving rotating cylinder electrodes”. *J. Appl. Electrochem.,* 22 (1992) 1161 – 1166.

13 E.M. Elsayed, A.E. Saba. “The electrochemical treatment of toxic hexavalent chromium form industrial effluents using rotating cylinder electrode cell”. *Int. J. Electrochem. Sci.*, 4 (2009) 627 – 639.

14 A.J. Chaundary, N.C. Goswami, S.M. Grimes. “Electrolytic removal of hexavalent chromium from aqueous solutions”. *J. Chem. Tech. Biotech.*, 78 (2003) 877 – 833.

15 G. Velasco-Martínez, S. Gutiérrez-Granados, A. Alatorre-Ordaz, I Rodríguez-Torres. “Analysis of the use of copper electrode in a filter-press electrochemical reactor for the electrochemical reduction of Cr(VI)”. *ECS Trans.*, 3 (2007) 57 – 65.

16 S. Velazquez Peña, C. Barrera Díaz, I. Linares-Hernández, B. Bilyeu, S. A. Martínez Delgadillo. “An effective electrochemical Cr(vi) removal contained in electroplating industry wastewater and the chemical characterization of the sludge produced”. *Ind. Eng. Chem. Research*, 51 (2012) 5909 – 5910.

17 E.C.W. Wijnbelt, L.J.J Janssen, “Reduction of chromate in dilute solution using hydrogen in a GBC-cell” *J. Appl. Electrochem*., 24 (1994) 1028 – 1036.

18 S. Goeringer, N.R. Tacconi, C.R. Chenthamarakshan, K. Rajeswar. “Reduction of hexavalent chromium by copper”. *J. Appl. Electrochem.*, 30 (2000) 891 – 897.

19 F.F. Rivera, C. Ponce de León, J.L. Nava, F.C. Walsh. The filter-press FM01-LC laboratory flow reactor and its applications. *Electrochim. Acta*, 163 (2015) 338 – 354.

20 G. Velasco-Martínez, S. Gutiérrez-Granados, I. Rodríguez-Torres, A. Alatorre-Ordaz. Study of Cr(VI) reduction in aqueous solutions at a glassy carbon electrode: Evidence of intermediary mechanisms in Applications of Analytical Chemistry in Environmental Research, pages 131-143. Research Signpost, Kerala, India, (2005), ISBN 81-308-0057-8.

21 A.T.S. Walker, A.A. Wragg, "The modelling of concentration-time relationships in recirculating electrochemical reactor systems". *Electrochim. Acta*, 22 (1977) 1129 – 1134.

22 F.C. Walsh, "A First Course in Electrochemical Engineering", The Electrochemical Consultancy, Romsey, (1993); ISBN 0-9517307-0-3.

23 G. Velasco-Martínez, S. Gutiérrez-Granados, A. Alatorre-Ordaz, I. Rodríguez-Torres, "Methodology for the Characterization of a Parallel-Plate Electrochemical Reactor". *ECS Trans.*, 3 (2007) 1 – 12.

24 J. Saien, A. Azizi, "Simultaneous photocatalytic treatment of Cr(VI), Ni(II) and SDBS in aqueous solutions: Evaluation of removal efficiency and energy consumption". *Process Saf. Environ. Prot.*, 95 (2015) 114 – 125.

25 K. Dermentzis, A. Christoforidis, E. Valsamidou, A. Lazaridou, N. Kokkinos, "Removal of hexavalent chromium from electroplating Wastewater by electrocoagulation with iron electrodes". *Global NEST J.*, 13 (2011) 412 – 418.

Figure captions

Figure 1 Schematic view of three-electrode electrochemical cell used in voltammetric and RDE studies.

Figure 2 a) An expanded view of the cell and b) an image of the individual parts of the flow cell.

Figure 3 Cyclic voltammetry at a titanium electrode at various Cr(VI) concentrations ($4 – 20 \times 10^{-3}$ mol dm^{-3}) + 0.1 mol dm^{-3} H_2SO_4, in the presence of dissolved oxygen; linear potential sweep rate, v = 100 mV s^{-1}.

Figure 4 Plot of the peak current density *vs*. the square root of the potential sweep rate, in the presence and the absence of oxygen at a titanium electrode in 2×10^{-3} mol dm^{-3} Cr(VI) + 0.1 mol dm^{-3} H_2SO_4, at 25 °C solution. Data taken from cyclic voltammetry curves at -0.45 V *vs*. Ag/AgCl.

Figure 5 Linear sweep voltammograms at potential sweep rate of, v = 5 mV s^{-1} on a titanium electrode (0.07 cm^2 area) in solution with 2.0×10^{-3} mol dm^{-3} Cr(VI) in 0.1 mol dm^{-3} H_2SO_4: a) in the absence of oxygen, b) in the presence of oxygen.

Figure 6 Limiting current density versus the square root of the rotation frequency for a titanium RDE during the reduction of Cr(VI) ions at different concentrations in 0.1 mol dm^{-3} H_2SO_4, in the absence of oxygen.

Figure 7 Electrode potential *vs.* current density curves for 2×10^{-3} mol dm^{-3} (100 mg dm^{-3}) of Cr(VI) ions in 0.1 mol dm^{-3} H_2SO_4 solution at titanium and graphite cathodes of 64 cm^2 area at different mean linear flow velocities in the presence of oxygen.

Figure 8 Percentage of Cr(VI) removal *vs* mean linear flow velocity after 60 minutes electrolysis using different cathodes: (◆) graphite at a potential of E = -0.65 V *vs.* Ag/AgCl and (▪) titanium at E = -1.0 V *vs.* Ag/AgCl.

Figure 9 Current efficiency (ϕ) and specific energy consumption ε_s at controlled flow velocities, using graphite and titanium cathodes at 60 minutes electrolysis.

Mean linear velocity, v / cm s^{-1}	**Current density, j / mA cm^{-2}**		**Cell voltage, E_{cell} / V**		**Mass transfer coefficient, k_m /cm s^{-1}**	
	Titanium	Graphite	Titanium	Graphite	Titanium	Graphite
10	0.916	0.839	1.90	2.29	1.4×10^{-3}	1.58×10^{-3}
25	1.755	1.602	1.95	2.34	2.77×10^{-3}	3.03×10^{-3}
45	2.365	2.060	1.98	2.37	3.56×10^{-3}	4.09×10^{-3}
60	2.975	2.441	2.0	2.42	4.22×10^{-3}	5.14×10^{-3}
80	3.51	2.670	2.01	2.46	4.61×10^{-3}	6.06×10^{-3}

Table 1 Current density j, electrolysis cell voltage (E_{cell}) and mass transfer coefficient at different mean linear electrolyte fluid velocities v, during the electrolysis of 2×10^{-3} mol dm^{-3} Cr(VI) ions in 0.1 mol dm^{-3} H_2SO_4, at constant cathode potential; -1.0 V *vs.* Ag/AgCl, on titanium and -0.65 V *vs.* Ag/AgCl on graphite.

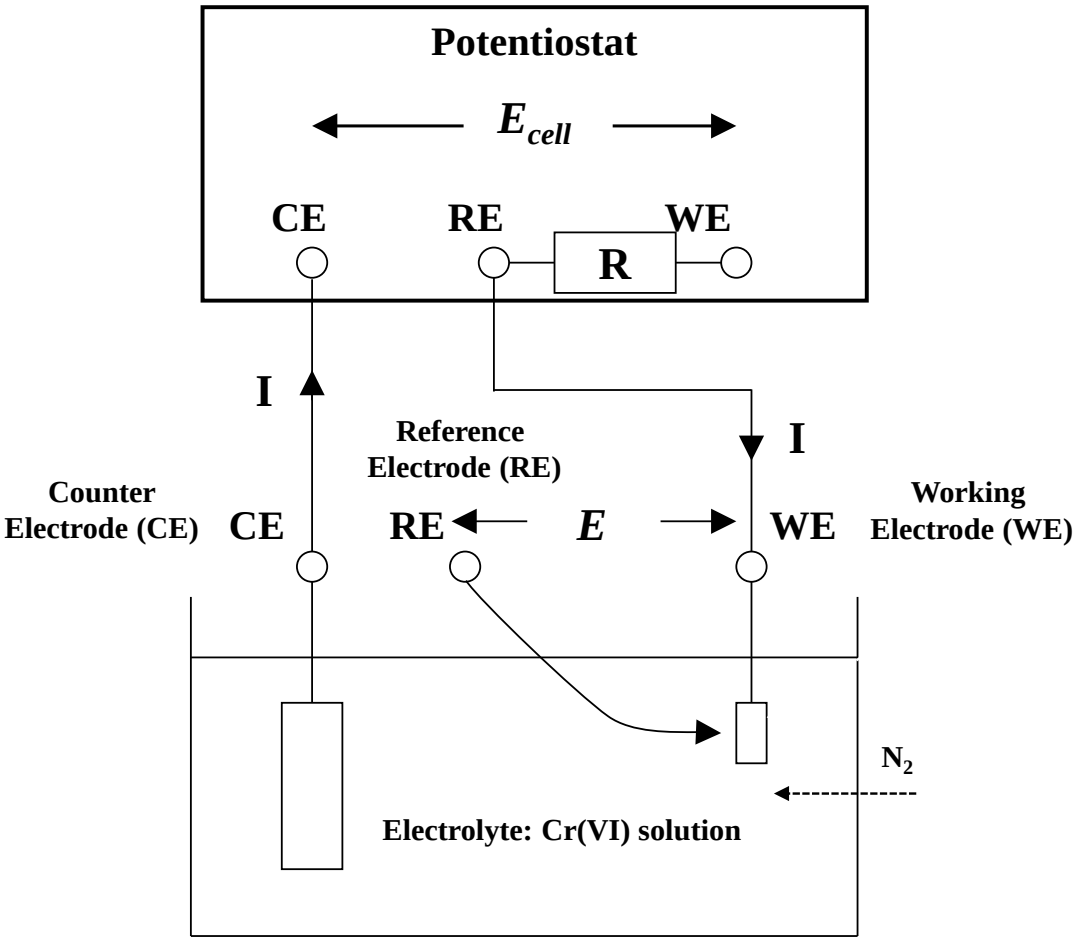
Potentiostat
E_{cell}
CE
RE
WE
R
I
I
Reference
Electrode (RE)
Counter
Electrode (CE)
CE
RE
E
WE
Working
Electrode (WE)
N_2
Electrolyte: Cr(VI) solution

Figure 1

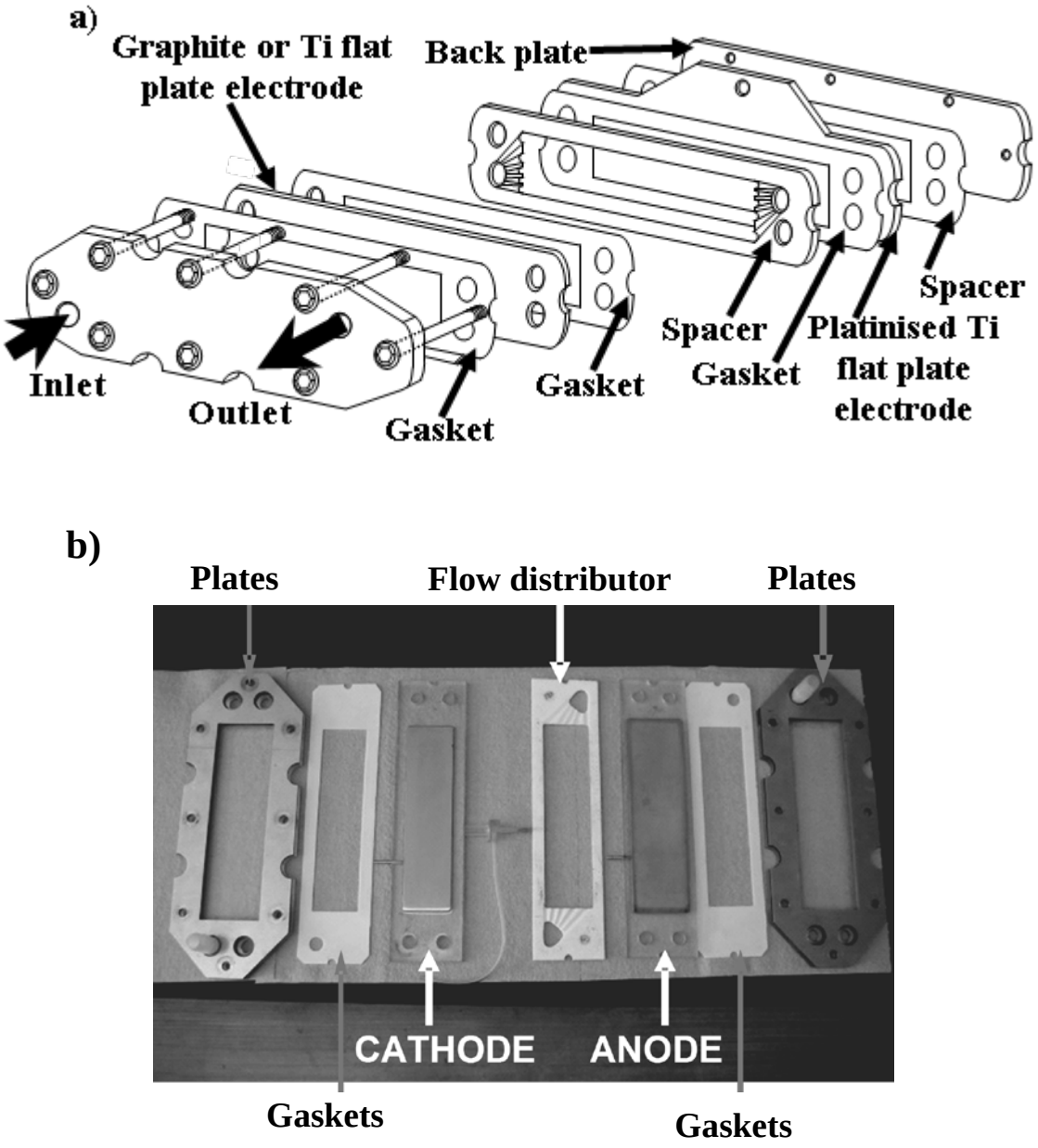
a)
Graphite or Ti flat plate electrode
Back plate
Spacer
Spacer
Gasket
Platinised Ti flat plate electrode
Inlet
Outlet
Gasket
Gasket
b)
Plates
Flow distributor
Plates
CATHODE
ANODE
Gaskets
Gaskets

Figure 2

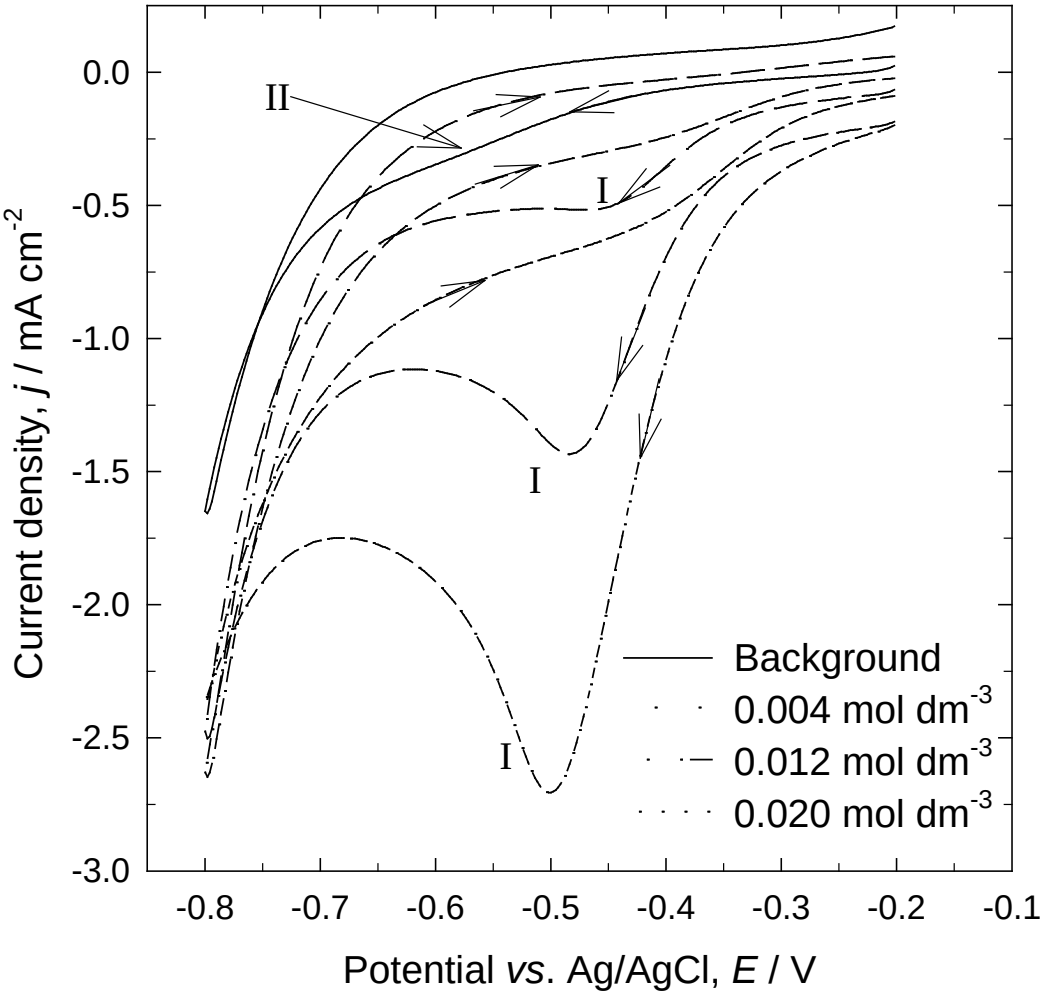
0.0
-0.5
-1.0
-1.5
-2.0
-2.5
-3.0
-0.8
-0.7
-0.6
-0.5
-0.4
-0.3
-0.2
-0.1
Current density, j / mA cm-2
Potential vs. Ag/AgCl, E / V
II
I
I
I
Background
0.004 mol dm-3
0.012 mol dm-3
0.020 mol dm-3

Figure 3

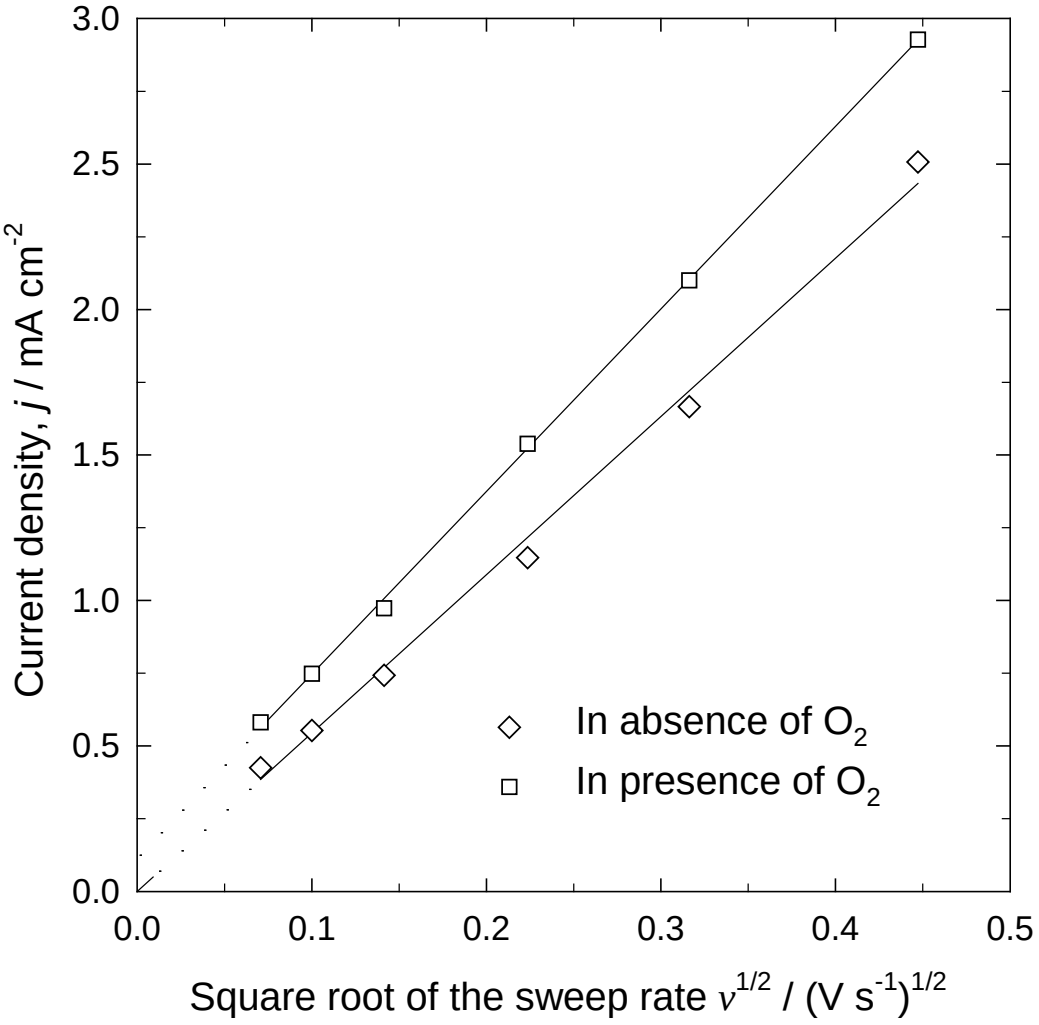
3.0
2.5
2.0
1.5
1.0
0.5
0.0
0.0
0.1
0.2
0.3
0.4
0.5
Current density, j / mA cm-2
Square root of the sweep rate v1/2 / (V s-1)1/2
In absence of O2
In presence of O2

Figure 4

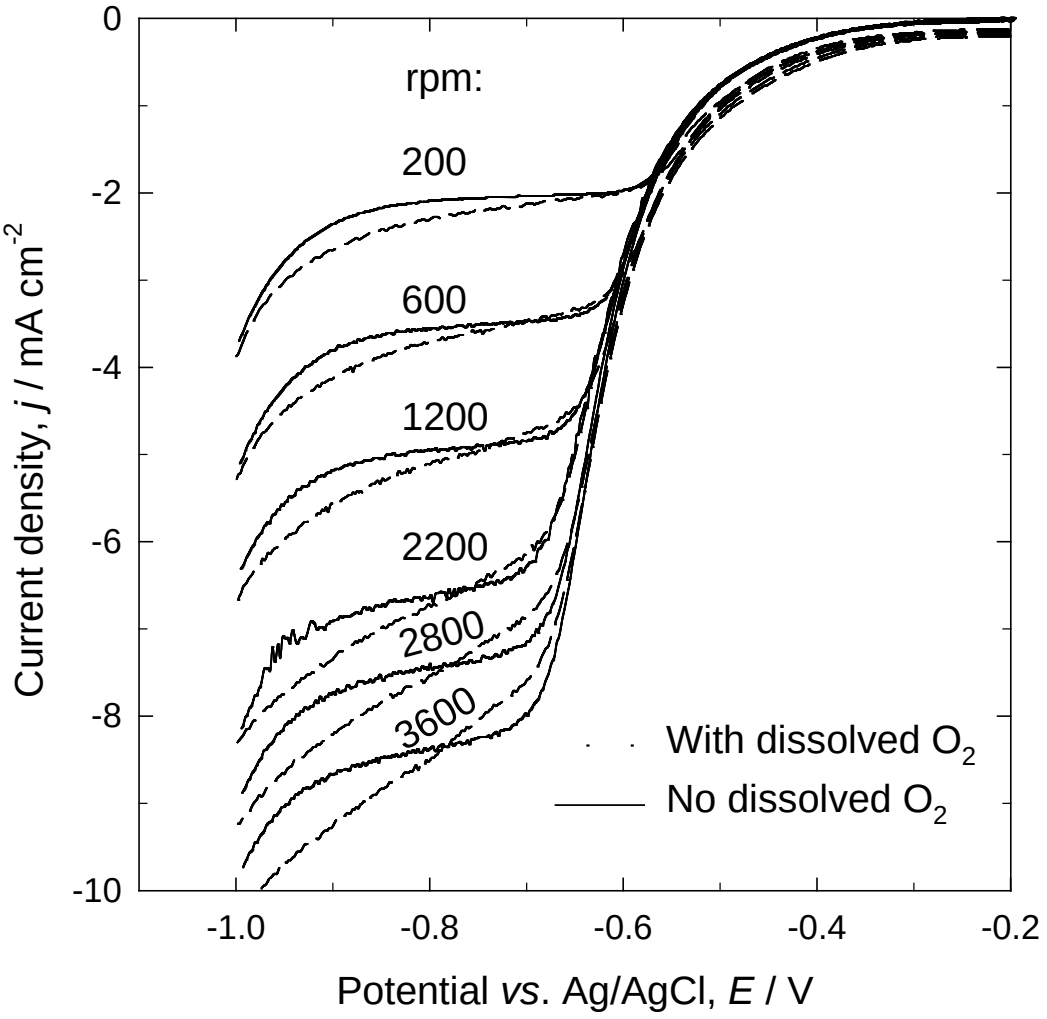
0
-2
-4
-6
-8
-10
-1.0
-0.8
-0.6
-0.4
-0.2
rpm:
200
600
1200
2200
2800
3600
With dissolved O2
No dissolved O2
Current density, j / mA cm-2
Potential vs. Ag/AgCl, E / V

Figure 5

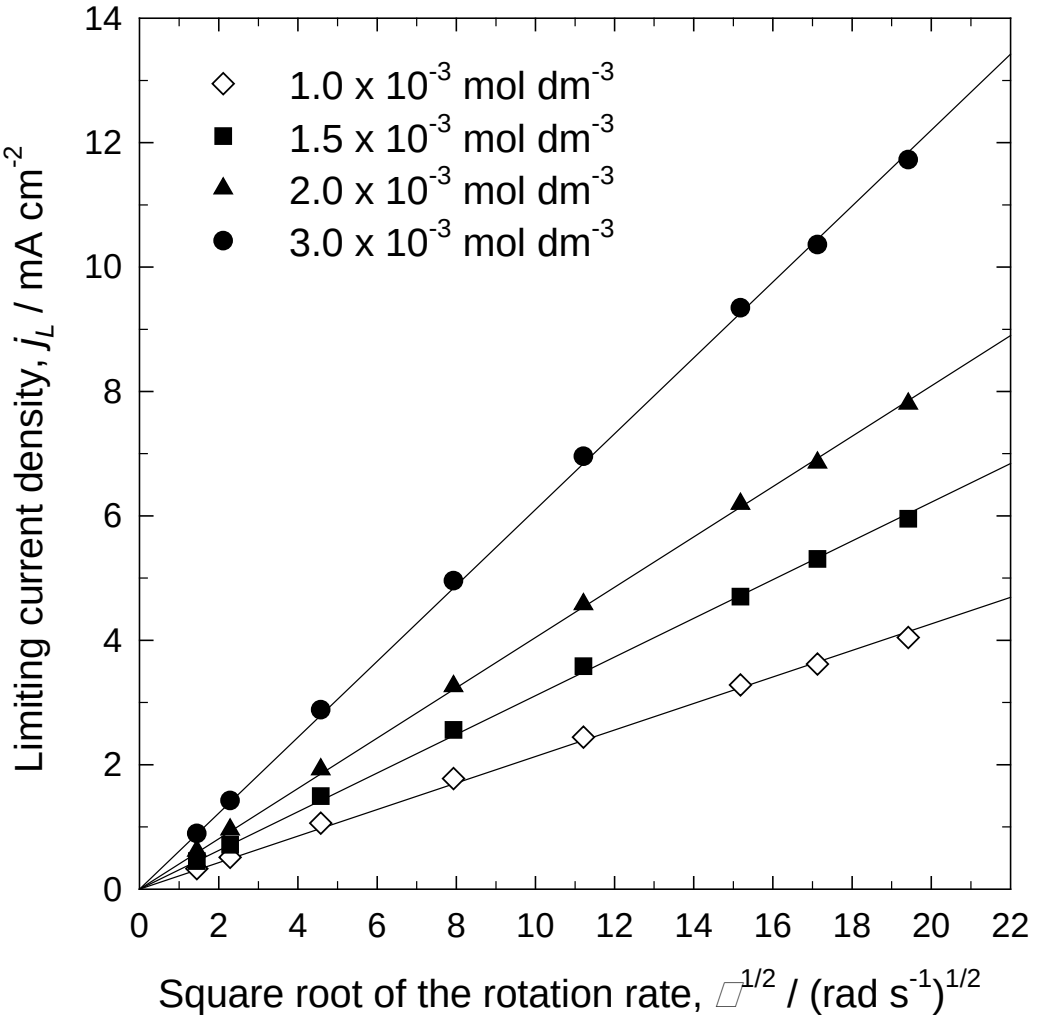
1.0 x 10-3 mol dm-3
1.5 x 10-3 mol dm-3
2.0 x 10-3 mol dm-3
3.0 x 10-3 mol dm-3
Limiting current density, jL / mA cm-2
Square root of the rotation rate, □1/2 / (rad s-1)1/2
0
2
4
6
8
10
12
14
16
18
20
22

Figure 6

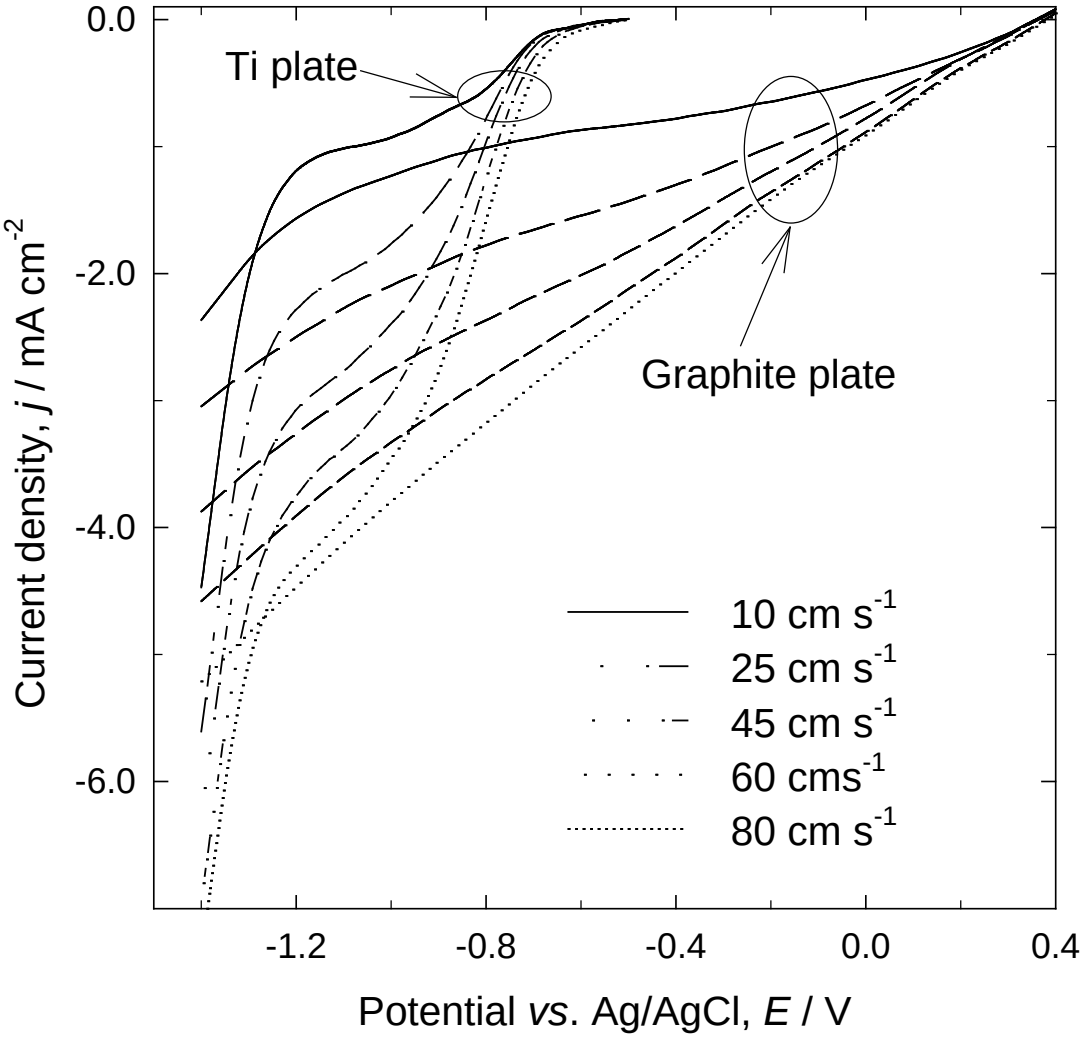
0.0
-2.0
-4.0
-6.0
Current density, j / mA cm-2
Ti plate
Graphite plate
10 cm s-1
25 cm s-1
45 cm s-1
60 cms-1
80 cm s-1
-1.2
-0.8
-0.4
0.0
0.4
Potential vs. Ag/AgCl, E / V

Figure 7

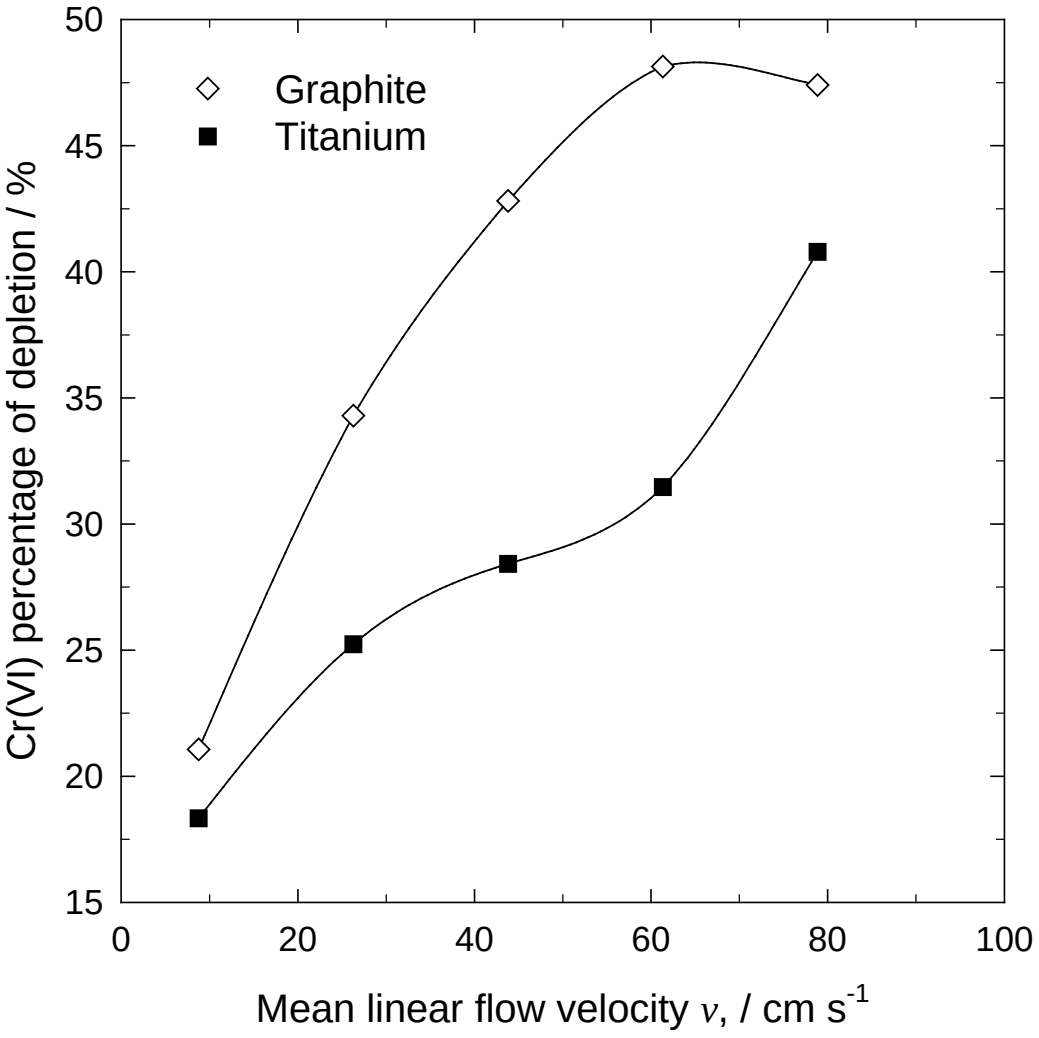
Graphite
Titanium
Cr(VI) percentage of depletion / %
Mean linear flow velocity v, / cm s-1
50
45
40
35
30
25
20
15
0
20
40
60
80
100

Figure 8

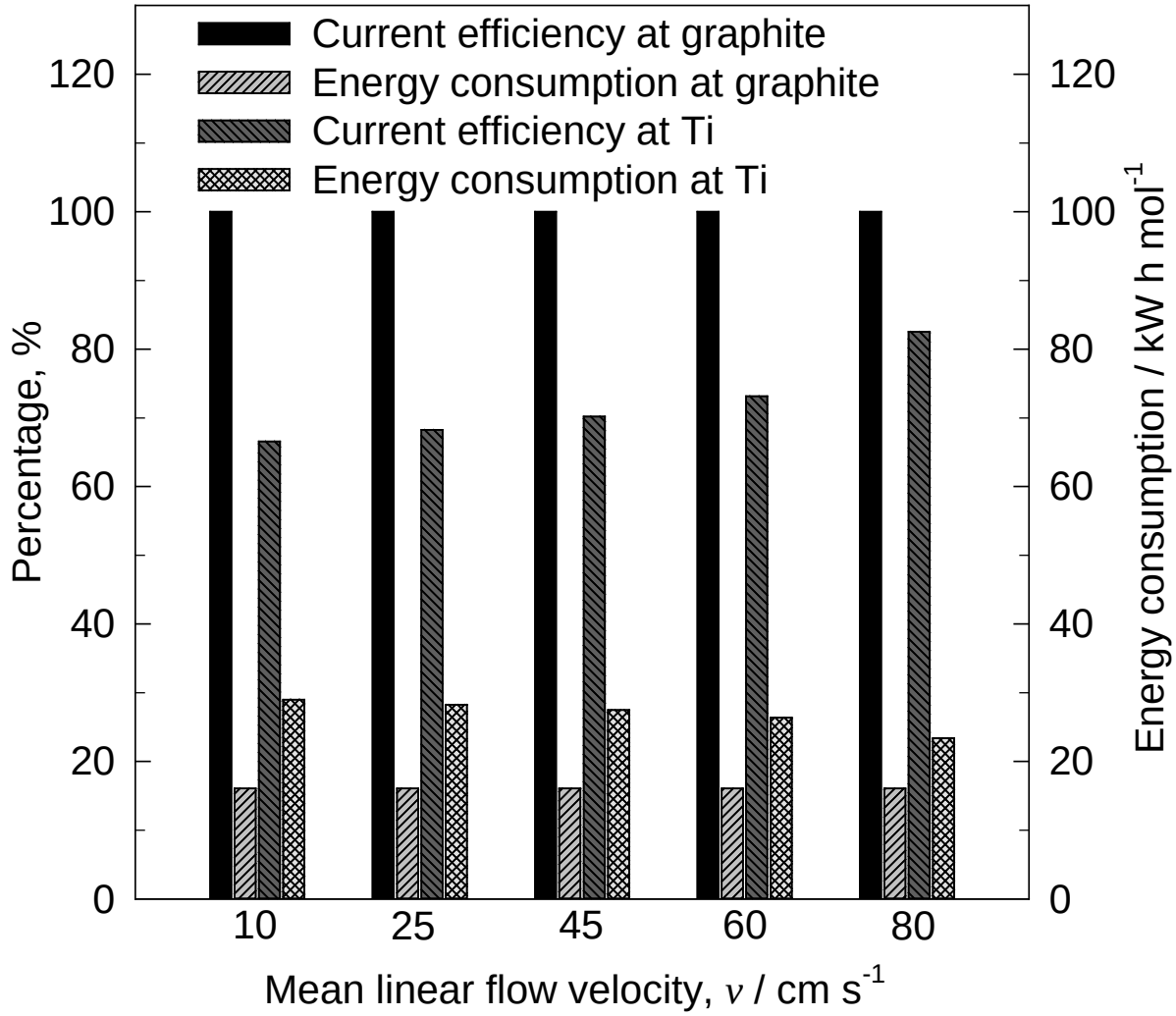
Current efficiency at graphite
Energy consumption at graphite
Current efficiency at Ti
Energy consumption at Ti
Percentage, %
Energy consumption / kW h mol-1
Mean linear flow velocity, v / cm s-1
0
20
40
60
80
100
120
10
25
45
60
80

Figure 9